Biochimica et Biophysica Acta 810 (1985) 252–268
Elsevier

BBA 41879

A mathematical model to study short-term regulation of mitochondrial energy transduction

Hermann-Georg Holzhütter, Wolfgang Henke, Wolfgang Dubiel and Gerhard Gerber

Institut für Physiologische und Biologische Chemie der Humboldt-Universität zu Berlin, Hessische straße 3–4, 104 Berlin (G.D.R.)

(Received May 24th, 1985)

Key words: Oxidative phosphorylation; Proton-motive force; ATP synthesis; Respiratory chain; Adenine nucleotide translocator; (Rat liver mitochondria)

A mathematical model is presented which includes the following elementary processes of mitochondrial energy transduction: hydrogen supply, proton translocation by the respiratory chain, proton-driven ATP synthesis by the F_0F_1-ATPase, passive back-flow of protons (leak) and carrier-mediated exchange of adenine nucleotides and phosphate. For these processes empirical rate laws are used. The model is applied to calculate time-dependent states of energy transduction in isolated rat liver mitochondria. From the general agreement of the computational results with experimental data (Ogawa, S. and Lee, T.M. (1984) J. Biol. Chem. 259, 10004–10011) the following conclusions can be drawn. (1) The length of the time interval during which mitochondria are able to maintain a relatively high and constant ΔpH in the absence of oxygen (anaerobiosis) is limited by the availability of intramitochondrial ATP. (2) The overshoot kinetics of ΔpH which appear when reoxigenating mitochondria after a preceeding anaerobiosis might be due to a lag phase kinetics of the F_0F_1-ATPase. (3) In phosphorylating mitochondria the homeostasis of ΔpH is brought about by a high sensitivity of the respiration rate and the rate of the F_0F_1-ATPase as to changes of ΔpH. (4) Analysis of the mean transient times shows that the rate of ATP synthesis in State 3 is controlled to almost the same extent by the hydrogen supply, the respiratory chain, the adenine nucleotide translocator and the proton leak.

Introduction

The linkage between transfer of reducing equivalents from any respiratory substrate to molecular oxygen and synthesis of ATP is the characteristic feature of mitochondrial energy transduction. Most of the enzymes and catalytic carriers which are involved in this vectorial metabolism are tightly integrated owing to their specific arrangement in the inner mitochondrial membrane.

In general, mathematical modelling may serve as a valuable tool to gain deeper insight into the function and regulation of complex metabolic systems [1,2]. With respect to mitochondrial energy transduction several mathematical models appeared in the literature [3–10,18]. All these models have in common that they are confined to steady states of the system whereas the model presented in this paper permits to study time-dependent regulation phenomena. Our model is based on the chemiosmotic concept of Mitchell [11], and includes the following elementary processes: hydrogen supply, proton translocation by the respiratory chain, intramitochondrial ATP synthesis by the F_0F_1-ATPase, passive back-flow of protons through

Abbreviation: Cyt, cytochrome.

the inner membrane and carrier-mediated exchange of phosphate and adenine nucleotides. In contrast to all previous models, magnesium-complex formation of the adenine nucleotides is taken into account. This is of importance, since magnesium-free ADP and ATP are exchanged via adenine nucleotide translocator [45], whereas Mg · ADP and Mg · ATP are the substrates of the F_0F_1-ATPase [46].

For the various enzymatic processes empirical rate laws are used. In particular, for the respiratory chain a rate law is proposed which reflects its function as a proton pump as well as the dependency of the apparent oxygen affinity on the redox state of the cytochrome a_3 system [5].

The kinetic parameters appearing in the rate laws are chosen in accordance with experimental data. Thus the model contains only very few 'free' parameters which are adjusted to obtain a good fit to the stimulated experiments.

Time-dependent solutions of the model equations are numerically calculated by solving a system of six ordinary non-linear differential equations with a Runge-Kutta-Fehlberg integration routine [25]. The computational results are compared with experimental data of oxygen-pulse experiments and State 3 experiments carried out by Ogawa and Lee [12]. From the good agreement between theoretical and experimental results it is suggested that the proposed model is well suited to describe nonequilibrium states of mitochondrial energy transduction. On the basis of the model the dynamical behaviour of the system can be better related to the kinetic mechanisms of its elementary components. In particular, our theoretical approach enables one to realize in a better way how the relative constancy of ΔpH (homeostasis) is achieved under extremely varying outer conditions, and to what extent the rate of ATP synthesis is controlled by the various steps of mitochondrial energy transduction.

The remaining discrepancies between computational results and experimental data may help to stimulate further experimental and theoretical work.

Description of the model

The various kinetic processes considered in our mathematical model are schematically represented in Fig. 1. As to the flow of energy within this system one may distinguish between three interacting subsystems: the redox system, characterized by the intramitochondrial $NAD^+/NADH$ ratio, involves the processes of hydrogen supply and utilization; the chemiosotic system is constituted by those chemical-cum-osmotic type processes which build up and utilize the proton-motive potential, $\Delta\mu_H$; the adenine nucleotide system is made up of those processes which affect the intra- and extramitochondrial phosphorylation potential $\Delta G_P = \log([ATP]/[H_2PO_4^-][ADP])$.

Redox system

The formation of intramitochondrial NADH is described by a simple first-order rate law. It is assumed that reduced substrate is available in a sufficiently high amount so that the rate of NADH production only depends on the concentration of NAD^+. In experiments on isolated mitochondria this condition is usually fulfilled.

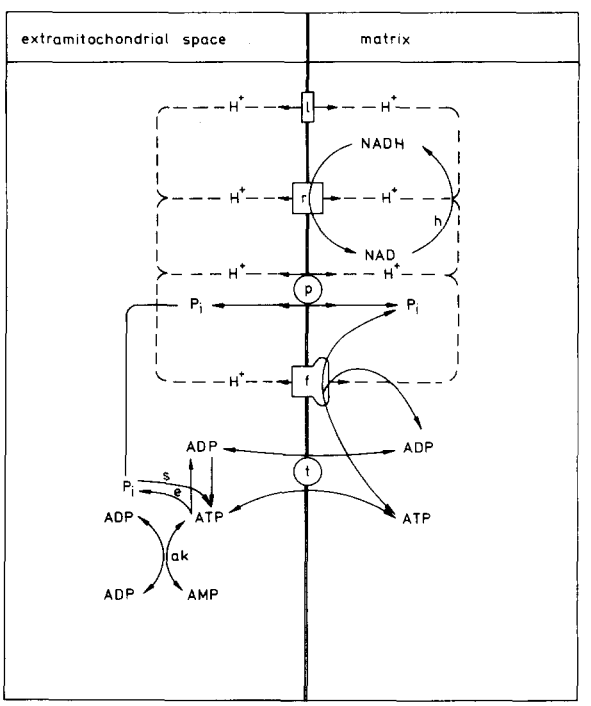

Fig. 1. Schematic representation of the reactions considered in the model. Abbreviations: h, hydrogen supply; r, respiratory chain; l, proton leak; f, F_0F_1-ATPase; p, phosphate transport; e, external ATP utilization; s, external ATP synthesis; t, adenine nucleotide translocator. The magnesium-complex formation of the adenine nucleotides is not shown.

In our calculations the value of the rate constant k_h was chosen such that in the resting state (state 4) the intramitochondrial $NAD^+/NADH$ ratio equals unity [13].

Chemiosmotic system

The redox system and the chemiosmotic system are linked by the respiratory chain. The overall reaction can be written as

$$SH_2 + \tfrac{1}{2}O_2 + n_r H_i^+ \rightarrow S + H_2O + n_r H_e^+ \qquad (1)$$

where n_r is the number of translocated protons per molecule NADH. The respiratory chain can be considered as a proton pump which is driven by a lateral electron flow due to the oxidation of any of a large number of respiratory substrates SH_2.

There is general agreement that proton extrusion appears at three coupling sites: site 1 (NADH-ubiquinone oxidoreductase), site 2 (ubiquinol-cytochrome *c* oxidoreductase) and site 3 (cytochrome *c* oxidase). Whereas the sites 1 and 2 form an equilibrium system, the formation of oxygen peroxid by the cytochrome *c* oxidase is highly exergonic and thus can be considered as the irreversible step [14].

These kinetic features are reflected by the binding scheme shown in Fig. 2. This scheme is similar to that proposed by Wilson et al. [5]. The essential difference is, however, that the Wilson model assumes a direct coupling between oxidation-reduction reactions and oxidative phosphorylation, whereas in our model the respiratory chain is treated as a proton pump responsible for the generation of ΔpH.

The rate law of the respiratory chain was derived from the binding scheme in Fig. 2 according to the rules of quasi-steady-state enzyme kinetics [1] (cf. legend of Fig. 2). With respect to oxygen this rate law can be written as a Michaelis–Menten equation with apparent maximum activity and K_M value being functions of the $NAD^+/NADH$ ratio and the proton gradient (ΔpH).

In Fig. 3 the theoretical respiration rate is plotted for various values of O_2, $NAD^+/NADH$ and ΔpH. It is seen that the respiration rate decreases very steeply with increasing ΔpH, and that the apparent affinity as to oxygen increases by about two orders of magnitude if ΔpH is

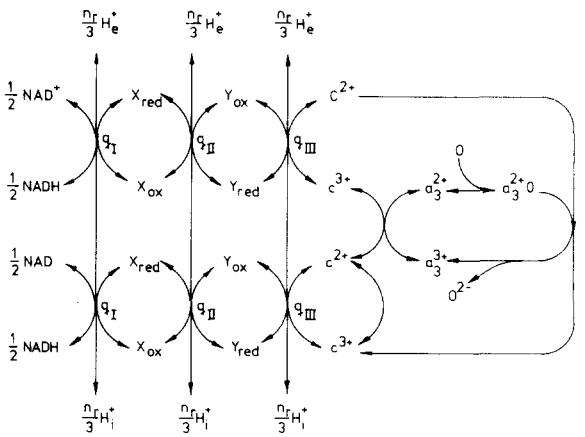

Fig. 2. Reaction scheme of the respiratory chain. Oxidation of one molecule NADH is coupled with the transfer of two electrons to cytochrome *c* and the extrusion of 3 $(n_r/3) = n_r$ protons. $X_{ox/red}$ and $Y_{ox/red}$ symbolize the oxidized and reduced electron-transferring subunits of site 1 and 2. One molecule Cyt c^{2+} causes the reduction of Cyt a_3 in a reversible step. When Cyt a_3 is reduced, oxygen can be bound. Then one electron of Cyt c^{2+} and one electron of Cyt a_3^{2+} are transferred to oxygen to form peroxide in an irreversible reaction step. The reversible reaction steps are described by the following equilibrium relations:

$$\frac{[c^{3+}]}{[c^{2+}]} = \phi = \frac{1}{\sqrt{q_i}} \sqrt{\frac{[NAD^+]}{[NADH]} \left(\frac{[H^+]_e}{[H^+]_i}\right)^{n_r}}$$

with

$$q_I = q_I \cdot q_{II} \cdot q_{III};$$

$$[a_3^{2+} \cdot O] = q_3 [a_3^{2+}][O];$$

$$\frac{[a_3^{2+}]}{[a_3^{3+}]} = q_2 \frac{[c^{2+}]}{[c^{3+}]}.$$

The rate of peroxide formation is given by

$$v_r = -\frac{d}{dt}[O] = k_r [a_3^{2+} \cdot O][c^{2+}].$$

If the algebraic equilibrium relations are used this rate can be written as

$$v_r = \frac{k_r [c][a_3][O]}{(1+\phi)\left(\frac{\phi + q_2}{q_2 q_3} + [O]\right)}$$

where $[c] = [c^{3+}] + [c^{2+}]$ and $[a_3] = [a_3^{3+}] + [a_3^{2+}]$. Estimation of the values for the equilibrium constants q_2 and q_3 from Ref. 34 shows that $\phi \gg q_2$. Hence the rate law B in Table I is obtained where the apparent constants k_r', p_r and q_r have the meaning $k_r' = k_r [c][a_3]$, $p_r = 1/\sqrt{q_i}$ and $q_r = \frac{1}{q_2 q_3}$.

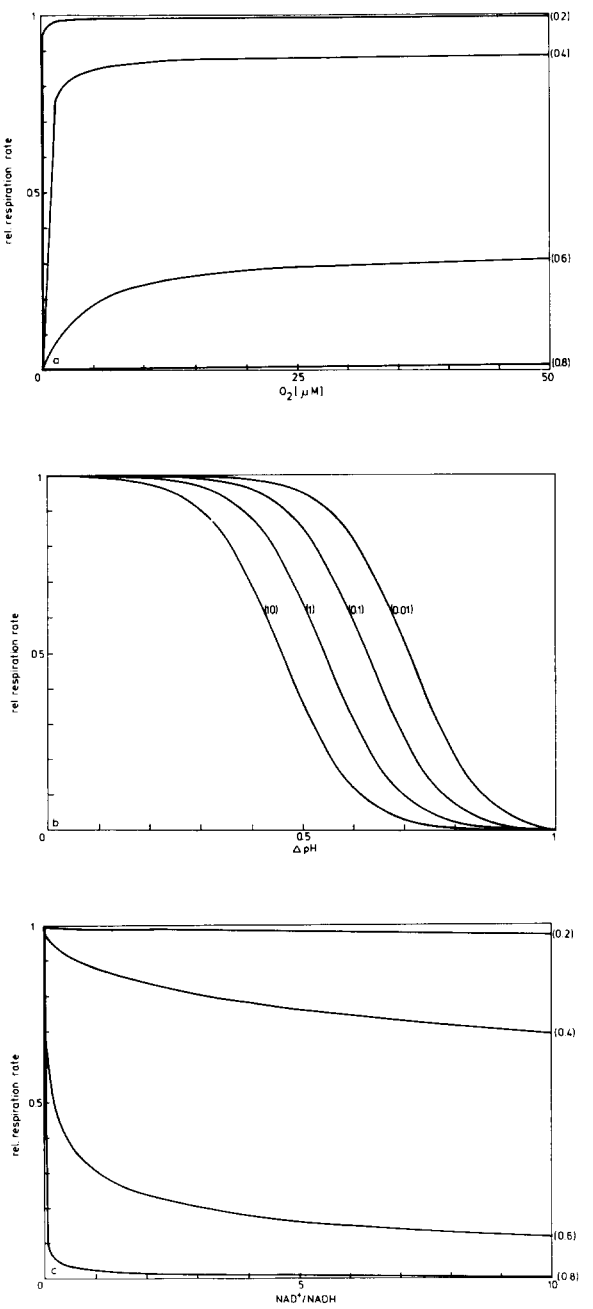

Fig. 3. Theoretical dependence of the respiration rate on oxygen concentration [O_2], redox ratio $NAD^+/NADH$ and ΔpH. The curves were calculated on the basis of the rate equation B in Table I. (a) Dependence on oxygen concentration for various values of ΔpH (values in parenthesis) and a redox ratio $NAD^+/NADH = 1$. (b) Dependence on ΔpH for various values of the redox ratio (values in paranthesis); $[O_2] = 230\ \mu M$. (c) Dependence on $NAD^+/NADH$ for various values of ΔpH (values in paranthesis); $[O_2] = 230\ \mu M$.

lowered from 0.8 to 0.2 (at constant $NAD^+/NADH = 1$). The value $n_r = 12$ was chosen, which corresponds to recent experimental findings [15].

The proton-leak represents the passive backflow of protons from the compartment with lower pH to the compartment with higher pH through the inner mitochondrial membrane. The rate law for this process is given by Eqn. C in Table I. The effective proton conductance C_M of coupling membranes was shown to be not greater than 0.11 μg ions of H^+/s per g mitochondrial protein [16] which corresponds to the value used in our model. With that value for C_M the respiration rate in the resting state amounts to about 10% of the State-3 respiration rate, which is in good agreement with experimental observations [17].

Secondary translocations of cations and anions is not explicitly considered in the model. Model computations of Reich and Rohde [18] and recent experiments of Duszynski et al. [19] have demonstrated that under steady-state conditions these secondary ion translocations give rise to a nearly constant relation between the electric potential $\Delta\psi$ and the osmotic potential $Z\,\Delta pH$, which both are components of the proton-motive potential $\Delta\mu_H$:

$$\Delta\mu_H = \Delta\psi - Z\,\Delta pH \tag{2}$$

With

$$\delta = \frac{-\Delta\psi}{Z\,\Delta pH} \tag{3}$$

it follows that

$$\Delta\mu_H = -(\delta + 1)Z\,pH \tag{4}$$

The constant δ has been used as an adjustable parameter of the model to assign to the proton-motive potential a value of $\Delta\mu_H = -180$ mV in the resting state. With that δ value the theoretical ratio $(\delta + 1)/\delta = 1.34$ is very close to the proportionality factor $\Delta\mu_H/\Delta\psi = 1.22$, determined by Duszynski et al. [19].

As far as proton translocation between extra- and intramitochondrial compartment is concerned the buffering power of both compartments is of importance. Within a small variation range of pH a linear relationship between the total proton con-

TABLE I
RATE EQUATIONS OF THE MATHEMATICAL MODEL

v_h, v_r, v_l, v_f, v_p and v_t, rates of hydrogen supply, respiratory chain, proton leak, F_0F_1-ATPase, phosphate transport and adenine nucleotide translocator, respectively. The kinetic parameters are listed in Table II. Abbreviations: $[X]_e$ and $[X]_i$, concentrations of metabolite X in the extramitochondrial and intramitochondrial compartment, respectively; [AMP], [ADP] and [ATP], concentrations of magnesium-free adenine nucleotides; [Mg·AMP], [Mg·ADP] and [Mg·ATP], concentrations of magnesium-complexed adenine nucleotides; [Mg] and $[Mg_t]$, concentrations of free and total magnesium; $[P^-]$, $[P^{2-}]$ and $[P_t] = [P^-]+[P^{2-}]$, concentrations of monovalent, divalent and total inorganic phpsphate; $[H^+]$ and $[H_t^+]$, concentrations of free and total protons

Equation number	Equation
A	$v_h = k_h[NAD^+]$
B	$v_r = \frac{v^r_{max}[O_2]}{K^r_M + [O_2]}$; $v^r_{max} = \frac{k'_r}{1+\phi}$; $K^r_M = q_r\phi$
	$\phi = p_r\left\{\frac{[NAD^+]}{[NADH]}\left(\frac{[H^+]_e}{[H^+]_i}\right)^{n_r}\right\}^{1/2}$
C	$v_l = C_M\frac{\Delta\mu_H}{Z}$
D	$v_f = V_f\left(1 - q_f\frac{[Mg\cdot ATP]_i}{[Mg\cdot ADP]_i[P^-]_i}\left[\frac{[H^+]_i}{[H^+]_e}\right]^{n_f(\delta+1)}\right)$
E	$v_p = V_p\left(1 - \frac{[P^-]_i}{[P^-]_e}\frac{[H^+]_i}{[H^+]_e}\right)$
F	$v_t = \frac{V_t\left([ATP]_i[ADP]_e - 10^{\Delta\psi/Z}[ATP]_e[ADP]_i\right)}{\left[K_0 + 10^{f_\psi\Delta\psi/Z}[ATP]_e + [ADP]_e\right]\left[K_0 + [ATP]_i + 10^{(1-f_\psi)\Delta\psi/Z}[ADP]_i\right]}$
	Equilibria:
	dissociation of monovalent phosphate: $pH = pK_a = \log\frac{[P^{2-}]}{[P^-]}$
G	$[P^-] = \frac{[P_t]}{1+q}$; $q = 10^{pH-pK_a}$
	magnesium-complex formation: extramitochondrial space
	$K_X = \frac{[Mg]_e[AXP]_e}{[Mg\cdot AXP]_e}$ (X = M, D, T)
	intramitochondrial space
H	$K_X = \frac{[Mg]_i[AXP]_i}{[Mg\cdot AXP]_i}$ (X = D, T)
	$K_R = \frac{[Mg]_i[R]_i}{[Mg\cdot R]_i}$
I	adenylate kinase reaction: $q_{ak} = \frac{[Mg\cdot ADP]_e[ADP]_e}{[Mg\cdot ATP]_e[AMP]_e}$

centration $[H_t^+]$ and the concentration of free protons $[H^+]$ can be assumed, i.e., $[H^+] = \beta[H_t^+]$. For the intramitochondrial space a buffering capacity of 22 μgions H^+ per pH unit per g protein was obtained from Mitchell and Moyle [16] in pulsed acid-base titration experiments. The buffering capacity of the extramitochondrial space depends on the corresponding experimental conditions, and thus has been used as a 'free' adjustable parameter of the model to obtain a good fit between calculated and measured variations of extramitochondrial pH.

Adenine nucleotide system

The adenine nucleotide system is linked with the chemiosmotic system by the mitochondrial

F_0F_1-ATPase which catalyses the reversible reaction

$$[Mg\cdot ADP]_i + [P^-]_i + n_f[H^+]_e \rightleftharpoons [Mg\cdot ATP]_i + n_f[H^+]_i \quad (5)$$

For the rate law of the F_0F_1-ATPase the rapid equilibrium approximation is used, since the rate of the ATPase exceeds by far the overall capacity of oxidative phosphorylation [20]. Under the assumption that a reaction proceeds in a near-thermodynamical equilibrium state the rate law can be approximated by

$$v = V(1 - e^{\Delta G/Z}) \quad (6)$$

where V is an apparent velocity and ΔG represents the free-energy change of the reaction [6]. For reaction 5 the free energy change is

$$\Delta G = \Delta G^0_P + Z \log \frac{[Mg\cdot ATP]_i}{[P^-]_i[Mg\cdot ADP]_i} + n_f \Delta\mu_H \quad (7)$$

Here ΔG^0_P denotes the (free-magnesium-corrected) standard phosphorylation potential, $\Delta\mu_H$ is the proton-motive potential defined by the relations 2 and 4, and n_f is the number of translocated protons per molecule ATP formed. Inserting Eq. 7 into Eq. 6 we arrive at the rate law Eqn. D (Table I).

For the rate law of the phosphate transporter also the rapid equilibrium approximation (Eqn. 6) is applied, since the influx of phosphate is very fast at 25°C [21]. The rate law Eqn. E (Table I) refers to the case that monovalent phosphate is cotransported with one proton [22]. The equilibrium between monovalent and divalent phosphate is described by a simple mass-action relation.

Mitochondrial ATP can be readily exchanged against cytosolic ADP by the adenine nucleotide translocator. The rate law Eqn. F (Table I) has been derived under the assumption that a ternary complex with one adenine nucleotide bound at both sides of the carrier performs the exchange in a single step. Such a mechanism is in accordance with recent kinetic studies of Duyckaerts et al. [23]. The difference between Eqn. F in Table I and the rate law used in Ref. 6 consists in the appearance of the additional terms $K_0/[ADP]_e$ and $K_0/[ADP]_i$ in the denominator. These terms are neglegible under saturating conditions which were a priori considered in Ref. 6

Besides the adenine nucleotide translocator, a second transport of adenine nucleotides across the inner membrane has been described, in the literature, which is responsible for the net uptake [48] and the depletion [49] of mitochondrial adenine nucleotides. Owing to its slowness this so-called net transport of adenine nucleotides is not taken into account in the model, since this paper only deals with short-term regulation phenomena.

The extramitochondrial adenine nucleotides AMP, ADP and ATP are related to each other by the adenylate kinase reaction

$$[Mg\cdot ATP]_e + [AMP]_e \rightleftharpoons [ADP]_e + [Mg\cdot ADP]_e \quad (8)$$

Since the capacity of the adenylate kinase is very high, it is presupposed in our model that reaction 8 is practically always in the thermodynamical equilibrium, i.e., a simple mass-action relation is used.

The formation of complexes between magnesium and adenine nucleotides is also described by mass-action equilibrium relations. Although the total intramitochondrial magnesium content is rather high (approx. 25 mM or more [40,41]) the concentration of free magnesium inside mitochondria was found to be less than 0.5 mM [12]. Therefore, binding of a considerable amount of intramitochondrial magnesium to any (not further specified) pool (R) has to be considered.

Mathematical equations

The reaction scheme shown in Fig. 1 corresponds to the following equation system:

$$\frac{d}{dt}[ADP_t]_i = -\frac{d}{dt}[ATP_t]_i = \mathscr{H}(v_t - v_f) \quad (9)$$

$$\frac{d}{dt}[P_t]_i = \mathscr{H}(v_p - v_f) \quad (10)$$

$$\frac{d}{dt}[NAD^+] = \mathscr{H}v_r - v_h \quad (11)$$

$$\frac{d}{dt}[2,1A]_e = mv_t \quad (12)$$

$$\frac{d}{dt}[H^+_t]_e = -\frac{m}{\mathscr{H}}\frac{d}{dt}[H^+_t]_i = m(n_r v_r - n_f v_f - v_t - v_p) \quad (13)$$

$$\frac{d}{dt}[P_t]_e = -mv_p \quad (14)$$

$$[P^{--}]_{i,e} = \frac{[P_t]_{i,e}}{1+10^{pH_{i,e}-pK_a}} \quad (15)$$

$$\frac{[ADP_t]_e[ADP_t]_e}{[ATP_t]_e[AMP_t]_e} = q_{ak}^*$$

$$= q_{ak}\frac{K_M(K_D+[Mg]_e)^2}{K_D(K_M+[Mg]_e)(K_T+[Mg]_e)} \quad (16)$$

$$[Mg]_e = \frac{[Mg_t]_e}{1+\sum_{X=M,D,T}\frac{[AXP_t]_e}{K_X+[Mg]_e}} \quad (17)$$

$$[Mg]_i = \frac{[Mg_t]_i}{1+\frac{[R]_i}{[Mg]_i}+\sum_{X=D,T}\frac{[AXP_t]_i}{K_X+[Mg]_i}} \quad (18)$$

TABLE II

PARAMETERS OF THE MODEL

Parameter	Value	Reference	Remark
k_h	0.9 min^{-1}	13	chosen such that NAD/NADH = 1 in the resting state
k_r'	150 nmol($\frac{1}{2}O_2$)·min^{-1}·mg^{-1}	17, 19	maximum (decoupler-stimulated) respiration
q_r	2 μM	34	calculated from the kinetic constants given in Ref. 34
p_r	$4\cdot10^{-4}$	5	estimated on the basis 15% reduction of cytochrome c in State 4
n_r	12	15	
C_M	9.6 μM·min^{-1}	16	
β_i	$6\cdot10^{-5}$	16	
β_e			adjustable parameter (given in the legends of figures)
V_f	350 nmol·min^{-1}·mg^{-1}		
q_f	10^9		$q_f = 10^{-\Delta G_P^0/Z}$ with $\Delta G_p^0 = -540$ mV (corrected for 1 mM free magnesium)
δ	2.95		chosen such that $\Delta\psi = -140$ mV in State 4
n_f	3	35	
V_p	200 nmol·min^{-1}·mg^{-1}	21	
V_t'	300 nmol·min^{-1}·mg^{-1}	36	
K_0	5 μM	37	
f	0.6	6	
Z	60 mV		
q_{ak}	0.25	38	
K_M	22.2 mM	39	
K_D	0.806 mM	39	
K_T	0.0813 mM	39	

Conservation quantities

$[\sum A]_i = [ADP_t]_i + [ATP_t]_i$	10 mM (oxygen-pulse type experiment 5 mM (State 3 experiment)
$[\sum A]_e = [AMP_t]_e + [ADP_t]_e + [ATP_t]_e$	chosen according to the experimental conditions
$[Mg_t]_i$	25 mM [40,41]
$[Mg_t]_e$	chosen according to the experimental conditions
$[NAD^+]+[NADH]$	3 mM [42]
[R]	18 mM

The maximum activities in Table II refer to 1 mg mitochondrial protein per 1 ml extramitochondrial space; hence the dilution factor $\mathcal{H} = 1\ ml/V_0$ occurs in the right-hand side of the differential equations 9–14, where m denotes the amount of mitochondrial protein (mg) and V_0 is the matrix volume.

According to the equilibrium relations (Eqn. H in Table I) the free and magnesium-liganded species can be expressed through the total concentrations. This was done by rewriting the adenylate kinase equilibrium in the form of Eqn. 16 and by deriving the self-consistent equations 17 and 18 for the external and internal concentration of free magnesium.

The two 'pool variables' $[\sum A]_e = [AMP_t]_e + [ADP_t]_e + [ATP_t]_e$ (sum of external adenine nucleotides which is a conservation quantity in the model) and $[2, 1A]_e = 2[ATP_t]_e + [ADP_t]_e$ have been introduced in order to eliminate the flux rate of the adenylate kinase from the right-hand side of the original differential equations according to the rules of quasi-steady-state approximation [24]. With the help of the algebraic equation [16] the external adenine nucleotides can be expressed by the above mentioned pool variables as

$$[ATP_t]_e = \frac{1}{2}\frac{q_{ak}\left(\left[\sum A\right]_e - [2, 1A]_e\right) + 4[2, 1A]_e}{4 - q_{ak}} \times \left(1 - \sqrt{1 - \frac{4(4 - q_{ak})[2, 1A]_e^2}{\left\{q_{ak}\left(\left[\sum A\right]_e - [2, 1A]_e\right) + 4[2, 1A]_e\right\}^2}}\right) \tag{19}$$

$$[ADP_t]_e = [2, 1A]_e - 2[ATP_t]_e \tag{20}$$

$$[AMP_t]_e = \left[\sum A\right]_e - [ADP_t]_e - [ATP_t]_e \tag{21}$$

The differential equation system (Eqns. 9–14) was solved numerically with a Runge–Kutta–Fehlberg fifth-order method [25] on a 60 K microcomputer (Silex). After each integration step the free magnesium concentrations $[Mg]_e$ and $[Mg]_i$ were computed by solving the self-consistent equations 17 and 18 with an iterative procedure [26].

Results

Simulation of oxygen-pulse-type experiments

Calculations have been performed to study the short-term regulation of mitochondrial energy transduction under conditions of varying oxygen supply. The computational results were compared with experimental data of ^{31}P-NMR experiments carried out by Ogawa and Lee [12].

The initial value problem is defined by the resting state of isolated rat liver mitochondria. The theoretical values for some important variables of the model obtained for the resting state are depicted in Table III. A good agreement of the theoretical values with experimental data is achieved. Pertubation of the initial state (State 4) was induced by complete and abrupt oxygen depletion at time $t = 0$ (i.e., putting $[O_2] = 0$). After 2 min of anaerobiosis the original oxygen concentration ($[O_2] = 230\ \mu M$) was reestablished to allow the system to return to its original steady state (State 4). The calculated time-dependent variations of external and internal pH, internal ATP and phosphate and $NAD^+/NADH$ are shown in Fig. 4–6.

During the anaerobic period the proton gradient is permanently lowered due to the proton leak. The decrease of the proton gradient occurs slowly during the first minute of anaerobiosis to become much more pronounced afterwards. The relative constancy of ΔpH during the initial phase of anaerobiosis is due to the dephosphorylation of intramitochondrial ATP by the F_0F_1-ATPase. Splitting of ATP by the F_0F_1-ATPase is associated with pumping of protons from the mitochondrial matrix to the extramitochondrial compartment which partially counteracts the lowering of the proton gradient. In other words, the chemical energy which is stored in ATP is converted back into chemiosmostic energy contained in the proton gradient. As long as a sufficient amount of internal ATP is available an 'energized state' of mitochondria is maintained which is characterized by a high and relatively constant ΔpH and $\Delta\mu_H$, respectively. This is illustrated in Fig. 7, where the time-dependent decline of ΔpH is shown to proceed faster with a decreasing amount of intramitochondrial adenine nucleotides.

The drop in ΔpH during anaerobosis according

TABLE III

COMPUTED AND MEASURED VALUES OF SOME VARIABLES IN STATE 4

The theoretical values were computed as stationary solutions of the differential equation system 9–14. The numerical integration was stopped if the values of all variables had reached a quasi-stationary state characterized by

$$\left|\frac{x_{i+1}-x_i}{x_i}\right| < \epsilon \ (\epsilon = 10^{-5}),$$

where x_i and x_{i+1} are the values of the variable x at the ith and the $(i+1)$th integration step. Initial values: $[\sum A]_e = 0$ (no adenine nucleotides in the extramitochondrial space), $[P_t]_e = 1$ mM, $[Mg_t] = 20$ mM; $[A]_i = 10$ mM, $[Mg_t]_i = 25$ mM, $[P_t]_i = 10$ mM. The concentration of intramitochondrial metabolites was calculated on the basis of a matrix volume $V_0 = 1.2$ μl/mg.

Quantity	Theoretical value	Experimental value	Ref.
v_r (nmol($\frac{1}{2}O_2$)·min^{-1}·mg^{-1})	2.3 [a]	10–13	12
		8.9	30
		15	19
ΔpH	0.82	0.86	30
		0.70	43
		0.80	12
$-\Delta\psi$ (mV)	145	150	12
		166	30
$[ATP_t]_i/[ADP_t]_i$	3.1	3–5	44
$[NAD^+]/[NADH]$	1	≈ 1	13
$[Mg]_i$ (mM)	0.31	< 0.5	12
$[P_t]_i$ (mM)	14	11	12

[a] The rather low value of the respiration rate is due to the fact that no (external or internal) ATP utilization is taken into account

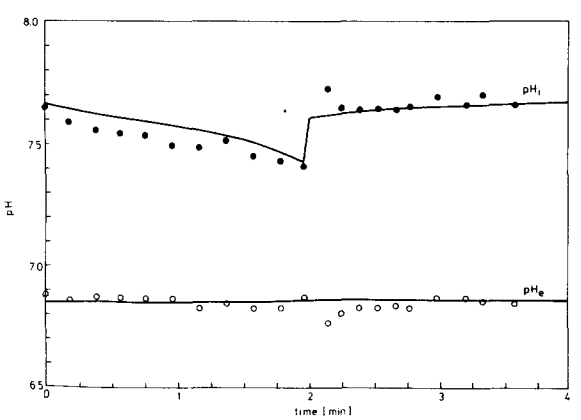

Fig. 4. Time-dependence of external and internal pH in an oxygen-pulse type experiment. The theoretical curves (solid lines) were calculated by putting the oxygen concentration $[O_2] = 0$ at $t = 0$ and by reestablishing the original oxygen concentration $[O_2] = 230$ μM at $t = 2$ min. The experimental points (●, pH_i; ○, pH_e) are taken from Ref. 12. Parameters: $\beta_e = 4 \cdot 10^{-4}$, $m = 40$ mitochondrial protein per ml, $\mathscr{H} = 800$ ($V_0 = 1.2$ μl/mg).

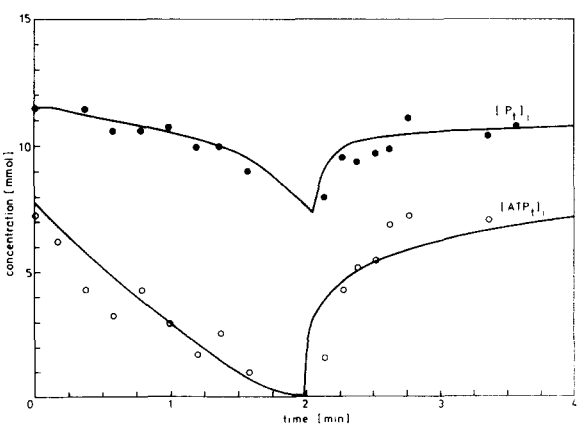

Fig. 5. Time dependence of internal ATP and inorganic phosphate in the oxygen-pulse type experiment described in the legend of Fig. 4. The experimental points (○, $[ATP_t]_i$; ●, $[P_t]_i$) are taken from Ref. 12. Since the theoretical phosphate concentrations are higher than the experimental values the calculated phosphate concentrations were multiplied with a constant factor 0.8 in order to match the experimental and theoretical initial values (at $t = 0$).

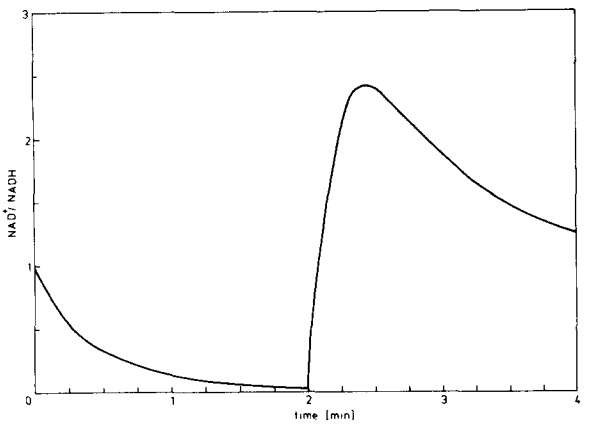

Fig. 6. Time-dependence of the intramitochondrial redox ratio $NAD^+/NADH$ in the oxygen-pulse type experiment described in the legend of Fig. 4.

to Eqn. E (Table I) is closely related to the drop in the intramitochondrial phosphate concentration (Fig. 5). It is interesting to note that the calculated and measured relative variations of internal phosphate are almost identical, whereas the absolute values differ in magnitude (cf. Table III). The curve in Fig. 5 was obtained by a simple scale transformation by multiplying the calculated values with a constant factor (0.8) to match the experimental and theoretical points at $t = 0$.

During anaerobiosis the $NAD^+/NADH$ ratio decreases monotonously from the initial value $NAD^+/NADH = 1$ to the low value $NAD^+/NADH = 0.03$ after 2 min of anaerobiosis. Such a

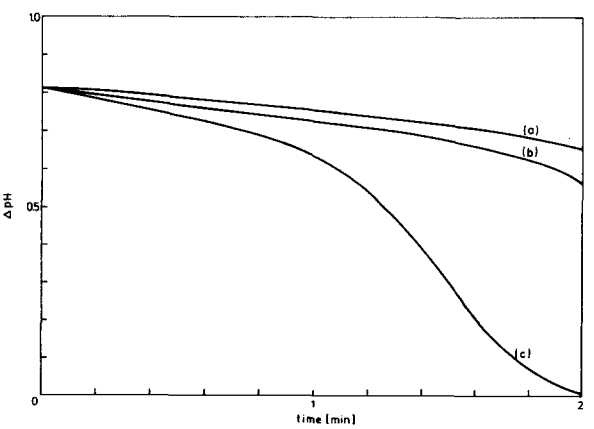

Fig. 7. Decline of the proton gradient (ΔpH) during 2 min of anaerobiosis (cf. legend of Fig. 4) for various intramitochondrial adenine nucleotide pools (a), $[\sum A]_i = 20$ mM; (b), $[\sum A]_i = 10$ mM; (c), $[\sum A]_i = 5$ mM.

steep decline is in accordance with experimental observations [13,27].

Onset of oxygen after 2 min of anaerobiosis leads to a very rapid increase of the proton gradient. Within 80 ms the internal pH is elevated from $pH_i = 7.42$ (at $t = 2$ min) to 7.63 (at $t = 0.0013$ min). After this very short time a quasi-equilibrium state has been reached where the utilization of the proton gradient by the leak, the phosphate transporter and the F_0F_1-ATPase is fully compensated by the respiratory chain. As the calculation reveals, the system now slowly moves towards the original steady state along the quasi-steady-state line $\frac{d}{dt}[H_t^+]_e = 0$.

The experimental points in Fig. 4 indicate an overshoot kinetics of ΔpH immediately after oxygenation. This kinetic phenomenon might be due to a delayed onset of any of the proton-driven processes when switching from anaerobic to aerobic conditions. Such lag phase kinetics are reported for the F_0F_1-ATPase which is known to undergo a slow conformational change bringing the enzyme from a state of ATP dephosphorylation to a state of ADP phosphorylation [28,29]. If this pecularity in the kinetic mechanism of the F_0F_1-ATPase is phenomenologically taken into consideration by increasing its maximum activity according to an exponential law, the calculated time-dependence of ΔpH exhibits an overshoot (Fig. 8a). The peak reaches a maximum at $\Delta pH = 0.88$ which lies even above the value in State 4 ($\Delta pH = 0.82$). This can be explained by the low $NAD^+/NADH$ ratio at the beginning of the aerobic period which (at the same values of $[O_2]$ and ΔpH as in State 4) gives rise to a higher respiration rate than in State 4 (cf. Fig. 3c). The hypothesis that the ΔpH overshoot might be due to a lag phase kinetics of the F_0F_1-ATPase is confirmed by the fact that the experimentally determined lag phase behaviour of intramitochondrial ATP can be reproduced in our calculations if a delayed activation of the F_0F_1-ATPase is taken into account (cf. Fig. 8b).

During the anaerobic period the $NAD^+/NADH$ ratio increases within 30 s from 0.03 to a maximum value of 2.5. Thereafter, the $NAD^+/NADH$ ratio relaxes slowly towards the steady state value $NAD^+/NADH = 1$.

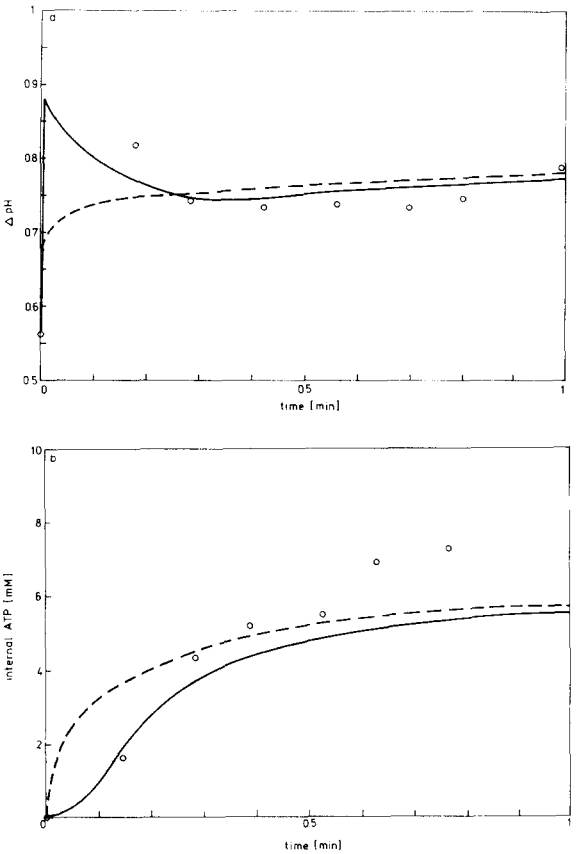

Fig. 8. Time-dependence of ΔpH (a) and internal ATP (b) after reoxigenation of isolated mitochondria which were exposed to a complete anaerobiosis for 2 min. The initial values of this calculation (at $t = 0$) are those obtained after 2 min anaerobiosis (cf. Fig. 4 and Fig. 5). At $t = 0$ the oxygen concentration was set to the original value $[O_2] = 230\ \mu M$. ———, lag phase kinetics of the F_0F_1-ATPase is taken into account in a phenomenological manner by increasing the maximum activity V_f exponentially, $V_f = V_{f_0}(1 - e^{-t/T})$, $V_{f_0} = 350$ nmol · min · mg, $T = 1$ min^{-1}; - - - - - -, without lag phase kinetics of the F_0F_1-ATPase, i.e., V_f = constant = V_{f_0}.

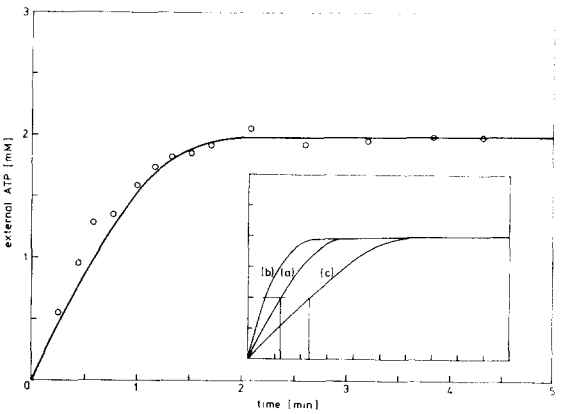

Fig. 9. Time-dependence of extramitochondrial ATP in a State 3 experiment. At $t = 0$ a State 4 → State 3 transition was induced by adding 2 mM ADP to the extramitochondrial space. The experimental points are taken from Ref. 12. Initial values: $[ADP_t]_e = 2$ mM, $[ATP_t]_e = [AMP_t] = 0$, $[P_t]_e = 3$ mM, $[Mg_t]_e = 20$ mM; $[\Sigma A]_i = 5$ mM, $[Mg_t]_i = 25$ mM. Parameters: $m = 65$ mitochondrial protein (mg) per ml, $\mathscr{H} = 650$ ($V_0 = 1.6\ \mu$l/mg). Inset: Calculated ATP formation in the State 3 experiment for various values of the maximum activity V_t of the adenine nucleotide translocator, (a) Normal activity, $V_t = V_{t_0} = 30$ nmol · min^{-1} · mg^{-1}; (b) increased translocator activity, $V_t = 2\ V_{t_0}$; (c) reduced translocator activity, $V_t = 0.5\ V_{t_0}$. The time needed to convert 50% of added ADP into ATP amounts to $t = 37$ s (a), $t = 20$ s (b) and $t = 70$ s (c).

Simulation of State-3 experiments

Calculations have been carried out to describe the time-dependent variation of model variables during the transient phase between State 4 and State 3.

Fig. 9 shows the time-course of ATP formation which is obtained if the steady State 4 is perturbated by adding 2 mM ADP to a suspension containing 60 mg mitochondrial protein per ml. The adenylate kinase was omitted in these calculations, since the incubation medium contained no magnesium in the corresponding NMR-experiment [12].

During State 3 the intramitochondrial ATP level drops down to about 25% of its value in State 4 (Fig. 10), the intramitochondrial ATP/ADP ratio decreases from 4 (in State 4) to a minimum value of 0.25. We note that the calculated variation of internal ATP is larger and the relaxation towards the new steady state proceeds slower than observed in the experiment. Changes of the internal ATP/ADP ratio between 3 (State 4) and 1 (State 3) are reported in the literature so that the calculated variations of this ratio lie in a reasonable range.

As shown in Fig. 11, the transition from the resting state to the active State 3 is connected with a relatively small decrease of ΔpH (and of $\Delta\psi$ and $\Delta\mu_H$ which are related to ΔpH by the linear relations [3] and [4]). The calculated minimum value of $\Delta\psi = -123$ mV in State 3 corresponds well to the measured value of $\Delta\psi = -115$ mV [12]. The fact that relatively small changes of the proton-

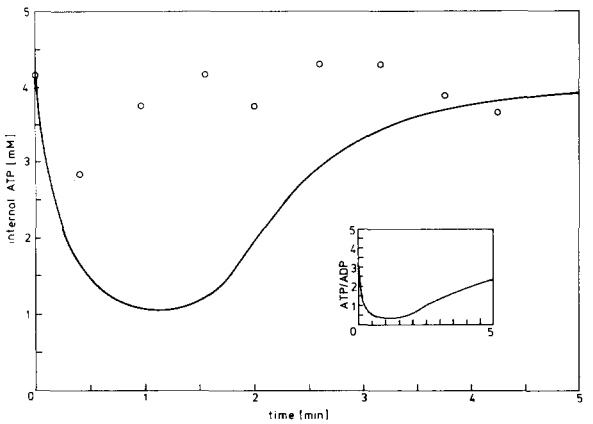

Fig. 10. Time-dependent variation of intramitochondrial ATP in the State 3 experiment described in the legend of Fig. 9. The experimental points are taken from Ref. 12. Inset: Time-dependent variation of the intramitochondrial ATP/ADP ratio.

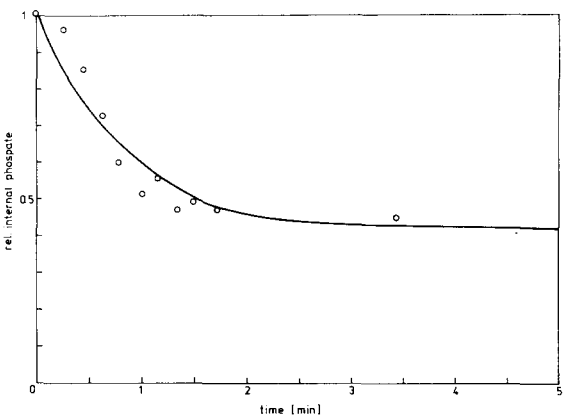

Fig. 12. Time-dependent variation of intramitochondrial phosphate in the State 3 experiment described in the legend of Fig. 9. Owing to the differences between the absolute theoretical and experimental values only by the relative concentration (i.e., all values referred to the initial value at $t = 0$) is plotted. The initial values are $[P_i] = 16.2$ mM (experiment) and 27 mM (theory).

motive force are associated with considerable changes of the respiration rate is in line with recent experiments of Duszynski et al. [19] who found a 90% inhibition of the respiration, while $\Delta\mu_H$ was changed only by 9%. This very high sensitivity of the respiration rate as to changes of $\Delta\mu_H$ is quantitatively well reflected by the rate law (Eqn. B in Table I) (cf. Fig. 3b).

The formation of external ATP is accompanied with a decrease of intramitochondrial phosphate (Fig. 12). Therefore, the new resting state is characterized by slightly different values of the model variables compared with the initial resting state (i.e., before ADP addition). This can be seen from the theoretical curves in Figs. 10 and 11. In particular, the intramitochondrial ATP does not reach the initial level and ΔpH approaches a new steady-state value of ΔpH 0.84, which is somewhat higher than the initial value of 0.82.

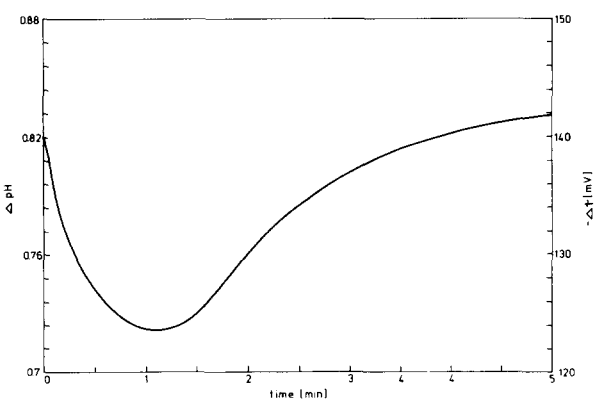

Fig. 11. Time-dependent variation of ΔpH ($\Delta\psi$) in the State 3 experiment described in the legend of Fig. 9.

In order to characterize the mean time which is needed by the variables of a dynamical system to reach a new steady state after a given pertubation, Heinrich and Rapoport [47] proposed the so-called mean (or characteristic) transient time

$$\tau_i = \frac{\int_0^\infty [S_i(t) - S_{i_0}]\, t\, dt}{\int_0^\infty [S_i(t) - S_{i_0}]\, dt} \qquad (22)$$

where $S_i(t)$ denotes the (time-dependent) ith variable of the system and $S_{i_0} = \lim_{t\to\infty} S_i(t)$ is its steady-state value. We have calculated the mean transient time for ADP phosphorylation in the State-3 experiment whereby the maximum activities of the elementary steps have been varied. As can be seen from Fig. 13 a significant dependency of the mean transient time on the maximum activities of (1) hydrogen supply, (2) respiratory chain, (3) adenine nucleotide translocator and (4) proton leak is obtained, whereas the variation of the max-

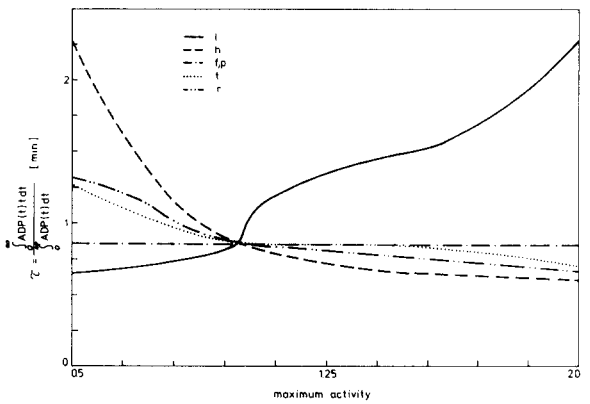

Fig. 13. Mean transient time for ADP phosphorylation in the State 3 experiment (described in the legend of Fig. 9) as a function of the maximum activity v^i_{max} of the ith elementary process. The indefinite integrals occurring in Ref. 22 were numerically computed according to the approximation formula

$$\int_0^\infty dx f(x) \approx I_n = \frac{\Delta t}{2}[f(x_0)+2f(x_1)+\ldots$$

$$+2f(x_{n-1})+f(x_n)],$$

where $\Delta t = t^*/n$ $(n = 200)$, $f(x_i) = f[x\{(i-1)\Delta t\}]$. The upper time limit t^* was chosen such that $|I_{n+1} - I_n| < 10^{-3}$. The maximum activities of the various transducers were varied between one-half and the double of their normal values.

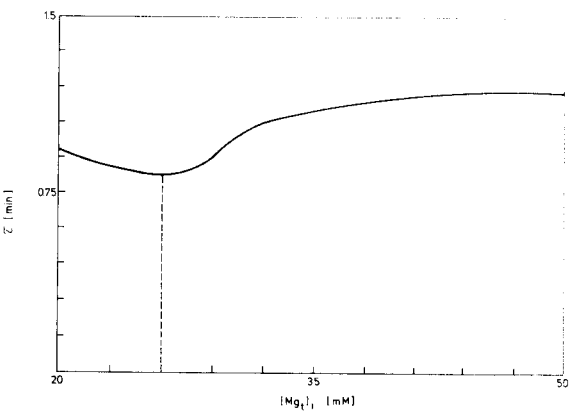

Fig. 14. Mean transient time for ADP phosphorylation in the State 3 experiment (described in the legend of Fig. 9) as a function of the intramitochondrial total magnesium content.

imum activities of the F_0F_1-ATPase and of the phosphate transporter practically does not change the value of the mean transient time. Hence it can be concluded that rate-limitation of ADP phosphorylation is excerted to almost the same extent by the processes (1)–(4). This result supports the theoretical and experimental finding in Refs. 7 and 20 that the control of oxidative phosphorylation is distributed between several elementary steps. But, whereas in Refs. 7 and 20 no control of oxidative phosphorylation in State 3 by the proton leak was found, our computations reveal a considerable rate limitation by this process.

In order to elucidate how the rate of oxidative phosphorylation is affected by the formation of magnesium complexes by the adenine nucleotides, the mean transient time for ADP phosphorylation in the State 3 experiment was calculated as a function of the total intramitochondrial magnesium content $[Mg_t]_i$ (Fig. 14). The calculation predicts a minimum value of τ (which corresponds to a maximum rate of oxidative phosphorylation) at a critical total magnesium concentration $[Mg_t]_i$ of 26 mM. Since the model is based on the assumption that a considerable portion of total magnesium is tightly bound to any intramitochondrial pools [R], it seems to be reasonable to introduce an 'effective' total intramitochondrial magnesium pool $[Mg_t^{eff}]_i = [Mg_t]_i - [R]$, which is accessible to the adenine nucleotides. We note that the critical value of the 'effective' intramitochondrial magnesium concentration at which τ reaches its minimum value amounts to an $[Mg_t^{eff}]$ value of 8 mM, and is thus in the range of the total intramitochondrial adenine nucleotide content $[\Sigma A]_i = 5$ mM.

Discussion

Several attempts have been made to understand more deeply the regulation of mitochondrial energy transduction on the basis of mathematical models.

Bohnensack et al. [6,7] set up a mathemathical model which involves the main elementary processes and which permits to calculate the steady states of the system. On the basis of this model the rate-controlling steps of oxidative phosphorylation in State 4 and State 3 of isolated rat liver mitochondria could be quantitatively identified [7,20].

Wilson and co-workers [3–5] regard the cytochrome *c* oxidase reaction of the respiratory chain

as the only regulatory step in oxidative phosphorylation. But in the light of modern control analysis [7,20,31] such a simplification is not justified. Moreover, the Wilson-models do not take into account explicitly the proton-motive force as a central energy intermediate.

Compared with these mechanistic models an alternative quantitative description of mitochondrial energy transduction is possible by application of non-equilibrium thermodynamics [8–10]. In these models a linear relationship between free-energy changes and fluxes is presupposed which is only valid if the underlying (mechanistic) rate laws can be approximated by linear functions as to the thermodynamical potentials.

The above-mentioned models have in common that they are confined to steady-state conditions, whereas our model is aimed to describe time-dependent state variations. The investigation of time-dependent states of a dynamical system provides a deeper insight into the function and regulatory structure of this system than obtainable by studying only its stationary states. Moreover, the need for a time-dependent approach results from the fact that in many experiments on isolated mitochondria non-steady state conditions are met (e.g., oxygen-pulse experiments, stop-flow experiments to measure the kinetics of fast exchange processes) which can be better interpreted by means of an appropriate theoretical approach.

In this paper we have restricted our considerations to the response of mitochondrial energy transduction to perturbations of the resting state induced by either variations of the oxygen supply or by changes of the extramitochondrial ATP/ADP ratio. From the good agreement of the computational results with experimental data it can be concluded that the proposed model is well suited to describe the rather complex system of mitochondrial energy transduction. It should be emphasized that this good agreement was achieved by varying only very few 'free' parameters of the model (δ, β_e, k_h), whereas the majority of the kinetic parameters was taken from independent sources. Nevertheless, some discrepancies between theory and experiment remain which cannot be abolished by parameter optimization only.

One of these open problems concerns the concentration of intramitochondrial inorganic phosphate. The calculated stationary concentrations are higher than the experimental values (even is it assumed that the mitochondria contain no phosphate before being incubated with the phosphate-containing incubation medium). These differences are possibly due to uncertainties in the determination of the intramitochondrial volume. Whipps and Halestrap [50] investigated carefully the effect of different incubation media on the matrix volume, and determined this volume to be $V_0 = 0.89$ μl/mg in the presence of mannitol (which was also present in the experiments [12]). We calculated the concentration of intramitochondrial metabolities on the basis of the higher values $V_0 = 1.2$ μl/mg (in the presence of 1 mM external phosphate) and $V_0 = 1.6$ μl/mg (in the presence of 3 mM external phosphate) which are given in ref. 12. If instead of these surprisingly high values a value $V_0 = 1$ μl/mg is assumed, the experimental values for the internal phosphate concentration are 13.2 mM (25.6 mM) in the presence of 1 mM (3 mM) external phosphate, and these values are very close to the theoretical values 14 mM (27 mM). Hence it could be possible that the experimental values for the internal phosphate concentration used throughout this paper are systematically too small. A further confirmation of this suggestion is the very good agreement between calculated and measured time-dependent variations of intramitochondrial phosphate (cf. Figs. 5 and 12) which is achieved when multiplying one type of values with a constant factor.

We have demonstrated that the overshoot characteristics of ΔpH observed immediately after reoxigenation of mitochondria (after a preceeding anaerobic period) can be explained by a lag phase kinetics of the F_0F_1-ATPase which is due to a slow conformational change of this transducer when switching from the dephosphorylating to the phosphorylating mode of action. It should be noted that this overshoot also can be reproduced in our calculations if any other (fast) proton-driven process exhibits such a lag phase kinetics. Therefore, further investigations are necessary to elucidate whether one (or a few) of proton-driven transducers of the inner mitochondrial membrane shows a certain time-delay before being fully active after abrupt changes of the mitochondrial state.

As shown in Fig. 10 the measured variation of

intramitochondrial ATP during the transitions State 4 → State 3 → State 4 is qualitatively reflected by the theoretical time dependency, but quantitative differences appear: the recovery of internal ATP proceeds slower than observed in the experiment. A similar discrepancy was obtained in the oxygen-pulse type experiment (cf. Figs. 5 and 8b). This difference is probably caused by the quasi-equilibrium rate law (Eqn. D. in Table I) for the F_0F_1-ATPase which certainly underestimates the $\Delta\mu_H$ dependency of this transducer under far-equilibrium conditions (which are actually met in State 3). A further reason for this quantitative difference might consist in the neglect of intramitochondrial guanine nucleotides in the model. As pointed out by Jacobus and Evans [32] the matrix nucleoside diphosphokinase may be involved in the buffering of the endogeneous adenylate energy charge.

Theoretical concepts have been developed [51,52] to characterize in a quantitative manner the relative importance of a distinct elementary process for the control of the steady-state fluxes of a biochemical system. As far as transient states of a system are concerned this control theory of steady states is not applicable. As a reasonable quantitative measure of the rate-limitation (or control) which is exerted by a given elementary process on the relaxation of any system variable towards its steady-state value the changes of the mean transient time (Eqn. 22) as to changes of the activity of the elementary process have been considered in this paper. This theoretical analysis (cf. Fig. 13) revealed four elementary processes to be involved in rate-control of oxidative phosphorylation during the transient process State 3 → State 4: hydrogen supply, respiratory chain, adenine nucleotide exchange and proton leak. Steady-state control analysis of oxidative phosphorylation in State 3 [7,20] did not provide evidence for a control by the proton leak. The different findings as to control of oxidative phosphorylation by the proton leak are obviously due to different time-scales of the State 3 experiment considered in Refs. 7 and 20 and in this paper. In order to apply the steady-state control theory on state-3, i.e., a time-dependent transient state, in refs. 7 and 20 only the initial part of the kinetic curves is considered which is characterized by a high and quasi-constant phosphorylation rate and rate of oxygen consumption, respectively. In contrast to such an initial rate analysis the mean transient time characterizes the whole time-course of the transient state. Since the post-initial (slow) phase of relaxation towards the steady state is mainly determined by the slow proton leak (while the other fast processes are in a quasi-equilibrium state) the regulatory importance of the proton leak is necessarily much more pronounced in our theoretical analysis than in the 'State 3 initial phase'-approach [7,20]. In other words, the regulatory importance of the proton leak increases considerably with increasing time during the State 3 → State 4 transition. This shows that the time-limitation exerted by one and the same elementary process may be different at different times of the transient process.

The mathematical model presented in this paper is based on Mitchell's chemiosmotic theory [1] which has as a central tenet the involvement of a proton electrochemical potential across the transducing membrane. The theoretical concept of a 'localized' chemiosmosis [33,53] which postulates the existence of a local force (e.g., local $\Delta\mu_H$) close the membrane which differs from the bulk aqueous phase $\Delta\mu_H$. Our model does not permit to discriminate between 'classical' and 'delocalised' chemiosmosis, since the interaction of protons with the corresponding transducers (respiratory chain, F_0F_1-ATPase, phosphate transporter) is not described in the framework of biochemical kinetics, but in terms of thermodynamical quantities such as ΔpH and $\Delta\ \mu_H$. One direction to improve mathematical modelling of mitochondrial energy transduction could therefore be to overcome this hybrid nature of current models between thermodynamics and kinetics. As stated by Mitchell [54] the time is ripe for a dynamically realistic modelling of the molecular mechanisms by which proton kinetics is related to other kinetic processes which are usually called to be 'proton-driven'.

Finally, it has to be pointed out that the proposed mathematical model contains some simplifications as far as $\Delta\psi$ and ΔpH are assumed to vary proportionally and the presently heavily discussed phenomena of non-ohmic proton leakage [57] and of slipping redox-driven proton pumps [58] are not considered.

The time-dependent variation of $\Delta\psi$ and ΔpH

was calculated under the assumption that the ratio between these two quantities is constant (δ) over the whole time-course studied. But deviations from the assumed constant ratio may occur within very short times $\Delta\tau$ (usually being much smaller than 1 s) if non-stationary transient states of the system are induced by sudden changes in the activity of the proton pumps [55,56]. Therefore, the computed time dependencies of $\Delta\psi$ and ΔpH might be incorrect within a time-interval $\Delta\tau$ around the time points where oxygen is added or removed, respectively, but this time-interval $\Delta\tau$ is expected to be much smaller than the distance between two subsequent data points which constitute the experimental curves of Ogawa and Lee [12,46]. Nevertheless, when applying the model to very fast short-term regulation processes proceeding with a critical time which is comparable with $\Delta\tau$, the relaxation of the electric and of the osmotic component of the proton-motive potential have to be separately described in the model by taking into account explicitly secondary ion translocations.

The experimental observation that under steady State 4 conditions the proton-motive potential $\Delta\mu_H$ and the respiration rate v_r are related to each other by a non-linear functional relationship led Nicholls [57] to the conclusion that the proton conductance of the inner membrane is not constant, but increases with increasing $\Delta\mu_H$, whereas Pietroben et al. [58] interprets this finding in terms of not tightly coupled proton pumps exhibiting a so-called molecular slipping. Although these two possible effects – non-ohmic proton leakage and molecular slipping – are not considered in the model, a good agreement between computational results and the experimental data of Ogawa and Lee [12,46] has been achieved. Therefore, further calculations simulating the experiments in Refs. 57 and 58 are necessary to elucidate, whether the model in its present form is sufficient to account for the non-linear relationship between $\Delta\mu_H$ and v_r or whether the model has to be refined and extended by taking into account either non-ohmic proton leakage or molecular slipping or both effects.

References

1 Heinrich, R., Rapoport, S.M. and Rapoport, T.A. (1977) Prog. Biophys. Molec. Biol. 32, 1–82

2 Garfinkel, D. (1981) Trends Biochem. Sci. 6, 69–71

3 Nishiki, K., Erecinska, M. and Wilson, D.F. (1978) Am. J. Physiol. 234, C73–C81

4 Erecinska, M., Wilson, D.F. and Nishiki, K. (1978) Am. J. Physiol. 234, C82–C89

5 Wilson, D.F., Owen, C.S. and Erecinska, M. (1979) Arch. Biochem. Biophys. 195, 494–504

6 Bohnensack, R. (1981) Biochim. Biophys. Acta 634, 203–218

7 Bohnensack, R., Küster, U. and Letko, G. (1982) Biochim. Biophys. Acta 680, 271–280

8 Stucki, J.W. (1979) in Energy Conservation in Biological Membranes (Schäfer, G. and Klingenberg, M., eds.), pp. 264–287, Springer-Verlag, Berlin

9 Van Dam, K. and Westerhoff, H.V. (1977) in Structure and Function of Energy-Transducing Membranes (Van Dam, K. and Van Gelder, B.F., eds.), pp. 157–161, Elsevier/North-Holland, Amsterdam

10 Westerhoff, H.V. and Van Dam, K. (1985) Non-Equilibrium Thermodynamics and Control of Energy Metabolism, Elsevier, Amsterdam

11 Mitchell, P. (1961) Nature 191, 144–148

12 Ogawa, S. and Lee, T.M. (1984) J. Biol. Chem. 259, 10004–10011

13 Klingenberg, M. and Slenczka, W. (1959) Biochem. Z. 331, 486–517

14 Erecinska, M. and Wilson, D.F. (1978) Trends Biochem. Sci. 3, 219–233

15 Pozzan, T., Di Virgilo, F., Bragadin, M., Miconi, V. and Azzone, G.F. (1979) Proc. Natl. Acad. Sci. USA 76, 2123–2127

16 Mitchell, P. and Moyle, J. (1967) Biochem. J. 104, 588–600

17 Aprille, J.R., Nosek, M.T. and Brennan, W.A. (1982) Biochem. Biophys. Res. Comm. 108, 834–839

18 Reich, J.G. and Rohde, K. (1983) Biomed. Biochim. Acta 42, 37–46

19 Duszynski, J., Bogucka, K. and Wojtczak, L. (1984) Biochim. Biophys. Acta 767, 540–547

20 Tager, J.M., Wanders, R.J.A., Groen, A.K., Kunz, W., Bohnensack, R., Küster, U., Letko, G., Böhme, G., Duszynski, J. and Wojtczak, L. (1983) FEBS Lett. 151, 1–8

21 Coty, W.A., and Pedersen, P.L. (1975) Mol. Cell. Biochem. 9, 109–124

22 Greenbaum, N.L. and Wilson, D.F. (1985) J. Biol. Chem. 260, 873–879

23 Duyckaerts, C., Sluse-Goffart, C.M., Fux, J.-P., Sluse, E.F. and Liebecq, C. (1980) Eur. J. Biochem. 106, 1–6

24 Tze-Fei Wong, J. (1977) Kinetics of Enzyme Mechanisms, Academic Press, London

25 Franco, R. and Canela, E.J. (1984) Int. J. Bio-Medical Computing 15, 419–432

26 Perrin, D.D. (1965) Nature 206, 170–171

27 Davies, E.J. and Blair, P.V. (1977) Biochem. Biophys. Res. Comm. 77, 1017–1023

28 Vasilyeva, E.A., Fitin, A.F., Minkov, I.B. and Vinogradov, A.D. (1980), Biochem. J. 188. 807–815

29 Sánchez-Bustamante, V.J., Darzon, A. and Gómez-Puyou, A. (1982) Eur. J. Biochem. 126, 611–616

30 Duszynski, J., Bogucka, K., Letko, G., Küster, U., Kunz, W. and Wojtczak, L. (1981) Biochim. Biophys. Acta 637, 217–223
31 Groen, A.K., Wanders, R.J.A., Westerhoff, H.V., Van der Meer, R. and Tager, J.M. (1982) J. Biol. Chem. 257, 2754–2757
32 Jacobus, W.E. and Evans, J.J. (1977) J. Biol. Chem. 252, 4232–4241
33 Williams, R.J.P. (1961) J. Theor. Biol. 1, 1–17
34 Wilson, D.F., Owen, Ch.S., and Holian, A. (1977) Arch. Biochem. Biophys. 182, 749–762
35 Lehninger, A.L. and Reynafarje, B. (1977) in Structure and Function of Energy-Transducing Membranes (Van Dam, K. and Gelder, B.F., eds.), pp. 95–106, Elsevier/North-Holland, Amsterdam
36 Stubbs, M. (1981) in Short-term Regulation of Liver Metabolism (Hue, L. and Van de Werve, G., eds.), pp. 411–425, Elsevier/North-Holland, Biomedical Press, Amsterdam
37 Souverijn, J.H.M., Huisman, L.A., Rosing, J. and Kemp, A. (1973) Biochim. Biophys. Acta 305, 185–198
38 Blair, J.M.D. (1970) Eur. J. Biochem. 13, 384–390
39 Lawson, J.W.R. and Veech, R.L. (1979) J. Biol. Chem. 254, 6528–6537
40 Hackenbrock, C.R., Rehn, T.G., Gamble, J.L., Weinbach, E.C. and Lemasters, J.J. (1971) in Energy Transduction in Respiration and Photosynthesis (Quagliarietto, E., Papa, S. and Rossi, C.S., eds.), pp. 285–305, Adriatica Editrice, Bari
41 Mittnacht, S., Sherman, S. and Farber, J.L. (1979) J. Biol. Chem: 254, 9871–9878
42 Sies, H. (1982) in Metabolic Compartmentation (Sies, H., ed.), pp. 205–226, Academic Press, London
43 Rottenberg, H. (1979) Methods Enzymol. 55, 547–569
44 Küster, U., Bohnensack, R. and Kunz, W. (1976) Biochim. Biophys. Acta 440, 391–402
45 Klingenberg, M. (1980) J. Membrane Biol. 56, 97–105
46 Ogawa, S. and Lee, T.M. (1982) Biochemistry 21, 4467–4473
47 Heinrich, R. and Rapoport, T.A. (1975) BioSystems 7, 130–136
48 Asimakis, G.K. and Aprille, J.R. (1980) FEBS Lett. 117, 157–160
49 Parce, J.W., Spach, P.I. and Cunningham, C.C. (1979) Biochem. J. 188, 817–822
50 Whipps, D.E. and Halestrap, A.P. (1984) Biochem. J. 221, 147–152
51 Kacser, H. and Burns, J.A. (1973) in Rate Control of Biological Processes (Davies, D.D., ed.), pp. 65–104 Cambridge University Press, London
52 Heinrich, R. and Rapoport, T.A. (1974) Eur. J. Biochem. 42, 97–105
53 Westerhoff, H.V., Melandri, B.A., Venturoli, G., Azzone, G.F. and Kell, D.B. (1984) FEBS Lett. 165, 1–5
54 Mitchell, P. (1985) J. Biochem. 97, 1–18
55 Mitchell, P. (1966) Chemiosmotic Coupling in Oxidative and Photosynthetic Phosphorylation, Glynn Research, Ltd., Bodmin, Cornwall
56 Westerhoff, H.V. and van Dam, K. (1979) Curr. Top. Bioenerg. 9, 1–62
57 Nicholls, D.G. (1974) Eur. J. Biochem. 50, 305–315
58 Pietrobon, D., Azzone, G.F. and Walz, D. (1981) Eur. J. Biochem. 117, 389–394